

# Finite-height effect on electron energy structure of lead salts nanorods

S.V. Goupalov

*Department of Physics, Jackson State University, Jackson, MS 39217 USA*

*and A.F. Ioffe Physico-Technical Institute,*

*26 Polytechnicheskaya, 194021 St. Petersburg, Russia*

## Abstract

The effect of the finite height of a cylindrical lead salt nanorod on its electronic structure is studied within the effective mass formalism. It is demonstrated that for most practical purposes it can be accounted for by sampling the subband dispersion dependencies of the infinite cylindrical quantum wire of the same radius at wave numbers  $k_z = \pi n_z/H$ , where  $H$  is the nanorod height and  $n_z$  is an integer. However, under certain conditions the otherwise degenerate electron energy levels will repel. A detailed account of these conditions is provided.

PACS numbers: 73.21.Hb,73.22.Dj,78.67.Lt

In recent years a significant progress has been made in solution-based synthesis of semiconductor nanostructures. As a result, a new class of nanostructures called nanorods has emerged [1]. The nanorods can be considered as an intermediate case between the quasi-zero-dimensional (0D) quantum dots and quasi-one-dimensional (1D) quantum wires and allow one to investigate the variation in material properties in the transition from 0D to 1D. They can be thought of as cylindrical semiconductor structures having diameter on the order of several nanometers and height up to several tens of nanometers.

Recently nanorods of lead salt semiconductors have been synthesized by a number of research groups [2–5]. Lead salt semiconductor compounds (PbS, PbSe, PbTe) are characterized by a large bulk exciton Bohr radius, in the range of 20 to 46 nm. Thus, in lead salt nanorods of a relatively short height, the strong confinement regime of charge carriers can be achieved in all three dimensions.

In Ref. [6] we have studied electronic structure of cylindrical lead salt quantum wires within the effective mass approximation. We found that the electron energy subbands of the conduction and valence bands in these quantum wires have monotonous dispersion dependencies. At first glance, in this situation the effect of finite dimension of the structure along the nanorod growth direction on the electron energy structure could be accounted for by substitution of the discrete values of wave numbers,  $\pi n_z/H$  (where  $H$  is the nanorod height and  $n_z$  is an integer) into energy dispersion dependencies for various subbands of the quantum wire. It turns out, however, that such procedure does not account for some qualitative changes in electron energy structure caused by the finite height of the nanorod. In this paper we will first describe these changes using a numerical solution of the effective mass equations, and then explain them based on the analytical dispersion equation derived in Ref. [6] for the case of a quantum wire.

The conduction and valence band extrema in lead salt semiconductors occur at the  $L$ -points of the Brillouin zone leading to the high valley degeneracy. Bartnik *et al.* have studied solutions of the effective mass equations customized for each of the four  $L$ -valleys for different quantum wire growth directions [7]. They showed that the valleys remain degenerate, within the effective mass approximation, when the growth occurs along the  $\langle 100 \rangle$  direction. It is not infrequent that lead salt nanorods grow along this crystallographic axis [4, 5, 7]. The valley

effective masses in this case still remain anisotropic. In what follows we will neglect this anisotropy and assume that the nanorods grow along the  $\langle 100 \rangle$  direction. Then the electron spectrum near the  $L$ -point taking into account only the two closely lying conduction and valence bands can be described by the spherical Dimmock model [6, 8]. In this model the electron wave function is written as

$$\Psi = \hat{u} |L_6^- \rangle + \hat{v} |L_6^+ \rangle, \quad (1)$$

where  $|L_6^- \rangle$  and  $|L_6^+ \rangle$  describe the Bloch functions while  $\hat{u}(\mathbf{r})$  and  $\hat{v}(\mathbf{r})$  are the spinors slowly varying with coordinates and satisfying the equation

$$\hat{H}(-i\nabla) \begin{bmatrix} \hat{u} \\ \hat{v} \end{bmatrix} = E \begin{bmatrix} \hat{u} \\ \hat{v} \end{bmatrix} \quad (2)$$

with

$$\hat{H}(-i\nabla) = \begin{bmatrix} \left(\frac{E_g}{2} - \alpha_c \Delta\right) & -iP(\boldsymbol{\sigma}\nabla) \\ -iP(\boldsymbol{\sigma}\nabla) & -\left(\frac{E_g}{2} - \alpha_v \Delta\right) \end{bmatrix}. \quad (3)$$

Here  $\sigma_\beta$  ( $\beta = x, y, z$ ) are the Pauli matrices,  $\alpha_c$ ,  $\alpha_v$ ,  $E_g$ , and  $P$  are parameters of the model and  $E$  is the electron energy. Eq. (3) is written using the system of units where  $\hbar = m_0 = e = 1$  ( $m_0$  and  $e$  are the mass and the charge of a free electron). Inclusion of the valley anisotropy would amount to introduction of longitudinal and transverse counterparts for the parameters  $P$ ,  $\alpha_c$ , and  $\alpha_v$  [7].

In order to solve Eq. (2) numerically for boundary conditions of cylindrical symmetry, one can first write down the Hamiltonian (3) in the basis of four cylindrically symmetric bispinors of the form

$$\Psi_1^{M,n}(\rho, \varphi, z) = \frac{e^{i(M-1/2)\varphi}}{\sqrt{2\pi}} f(z) C_{M-1/2,n} J_{M-1/2} \left( x_{M-1/2,n} \frac{\rho}{R} \right) \begin{bmatrix} 1 \\ 0 \\ 0 \\ 0 \end{bmatrix},$$

$$\Psi_2^{M,n}(\rho, \varphi, z) = \frac{e^{i(M+1/2)\varphi}}{\sqrt{2\pi}} f(z) C_{M+1/2,n} J_{M+1/2} \left( x_{M+1/2,n} \frac{\rho}{R} \right) \begin{bmatrix} 0 \\ 1 \\ 0 \\ 0 \end{bmatrix},$$

$$\Psi_3^{M,n}(\rho, \varphi, z) = \frac{e^{i(M-1/2)\varphi}}{\sqrt{2\pi}} f(z) C_{M-1/2,n} J_{M-1/2} \left( x_{M-1/2,n} \frac{\rho}{R} \right) \begin{bmatrix} 0 \\ 0 \\ 1 \\ 0 \end{bmatrix},$$

$$\Psi_4^{M,n}(\rho, \varphi, z) = \frac{e^{i(M+1/2)\varphi}}{\sqrt{2\pi}} f(z) C_{M+1/2,n} J_{M+1/2} \left( x_{M+1/2,n} \frac{\rho}{R} \right) \begin{bmatrix} 0 \\ 0 \\ 0 \\ 1 \end{bmatrix}.$$

Here  $R$  is the radius of the cylindrical nanostructure,  $x_{L,n}$  is the  $n$ th zero of the Bessel function,  $J_L(x)$ , and

$$C_{L,n} = \frac{\sqrt{2}}{R |J_{L+1}(x_{L,n})|}$$

is the normalization coefficient. All these bispinors are characterized by the quantum number  $M$ , the projection of the total angular momentum onto the growth direction,  $z$ , and vanish on the cylindrical surface of the nanostructure.

For a cylindrical quantum wire the function  $f(z)$  should be chosen in the form of a plane wave

$$f(z) = \frac{e^{ik_z z}}{\sqrt{2\pi}}.$$

If the index  $n$  runs from 1 to  $n_{max}$ , then the Hamiltonian (3) written in the chosen basis, for given quantum numbers  $M$  and  $k_z$ , represents a  $4 n_{max} \times 4 n_{max}$  matrix. If one is interested in a certain number of subbands characterized by the given value of the total angular momentum projection,  $M$ , it is enough to set  $n_{max}$  equal to that number. One can check that numerical diagonalization of the resulting Hamiltonian leads to electron energy dispersion dependence coinciding (with a very high precision) with that obtained from solution of the dispersion equation derived analytically and given by Eq. (25) of Ref. [6]. The numerical procedure is very robust and for practical calculations it would be our first choice.

For a nanorod of height  $H$  the function  $f(z)$  can be chosen in the form

$$f(z) = \sqrt{\frac{2}{H}} \sin \frac{\pi n_z z}{H}. \quad (4)$$

If the index  $n_z$  runs from 1 to  $n_z^{max}$  then the Hamiltonian (3), for a given quantum number  $M$ , represents in the chosen basis a  $4 n_{max} n_z^{max} \times 4 n_{max} n_z^{max}$  matrix. We have numerically

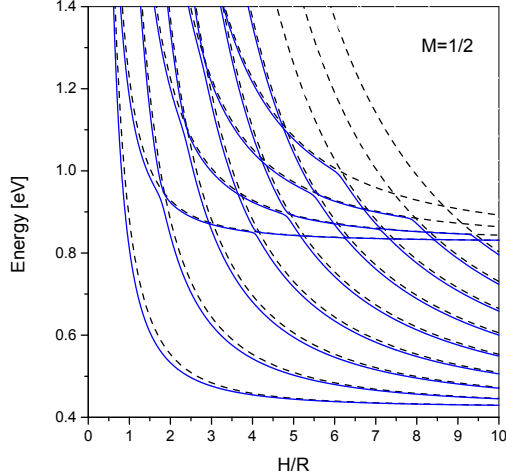


FIG. 1: (Color online) Energies of levels of size quantization described by the quantum number  $M = 1/2$  in a PbSe nanorod of radius  $R = 20 \text{ \AA}$  and height  $H$  as functions of  $H/R$  (solid lines). Dashed lines: energy dispersion  $E_{1/2, n_c}(k_z)$  for subbands of a PbSe cylindrical quantum wire of radius  $R = 20 \text{ \AA}$  for quantum numbers  $M = 1/2$ ,  $n_c = 1, 2$  [6] calculated at  $k_z = \pi n_z/H$ .

diagonalized this matrix for nanorod radius  $R = 20 \text{ \AA}$  and nanorod heights in the range from  $10 \text{ \AA}$  to  $200 \text{ \AA}$ . We used the same material parameters as in Ref. [6] (corresponding to PbSe nanorods) and the values of  $n_{max} = 3$ ,  $n_z^{max} = 30$ . In Fig. 1 by solid lines are shown the dependencies of the first 10 eigenvalues occurring within the conduction band and corresponding to the quantum number  $M = 1/2$  on the height to radius ratio,  $H/R$ . By dashed lines in Fig. 1 are shown the quantum wire subband energies [6]  $E_{1/2, n_c}(k_z)$  calculated at  $k_z = \pi n_z/H$  for a PbSe quantum wire of radius  $R = 20 \text{ \AA}$ .

The fact that the solid lines in Fig. 1 closely follow the dashed ones suggests that the quantum number  $n_z$  and the wave function (4) represent a good zero-order approximation to describe the motion along the nanorod growth direction,  $z$ . On the other hand, one can see that the dependencies of nanorod energy levels presented in Fig. 1 demonstrate both crossings and anti-crossings (or avoided crossings). In order to reveal the underlying pattern some regions of Fig. 1 are presented in Figs. 2 and 3 on an enlarged scale. These figures reveal that the level crossings and anti-crossings form a checker-board pattern, although the anti-crossings become less pronounced as the nanorod height increases. The same situation occurs for other values of  $M$ , as demonstrated in Fig. 4 for  $M = 3/2$ . In Fig. 5 the levels

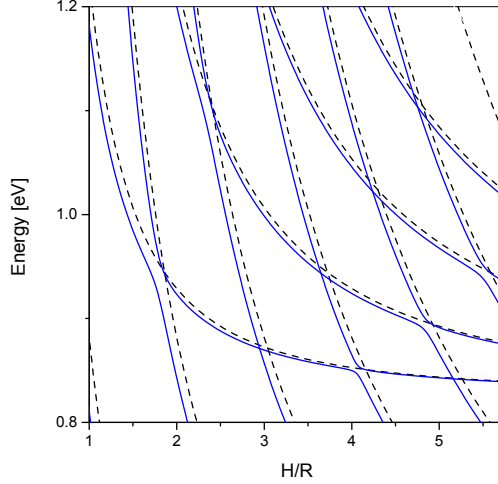


FIG. 2: (Color online) Same as Fig. 1 but on an enlarged scale.

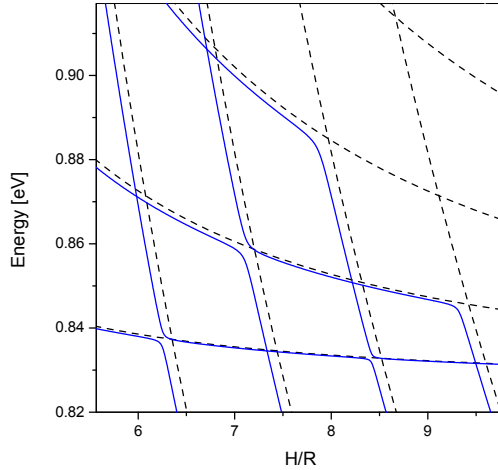


FIG. 3: (Color online) Same as Fig. 1 but on an enlarged scale.

for  $|M| = 1/2$  and  $|M| = 3/2$  are plotted together to account for lowest conduction band energy levels in nanorods.

The occurrence of the checker-board pattern of crossings and anti-crossings in the height dependence of electron energy levels in lead salts nanorods can be understood if one analyzes the equation describing electron energy dispersion in lead salts quantum wires [6]. This equation is given by Eq. (25) of Ref. [6]. For a given value of the quantum number  $M$  it has the following structure

$$k_z^2 A + B C = 0. \quad (5)$$

When  $k_z = 0$  Eq. (5) breaks into two separate equations  $B = 0$  and  $C = 0$  describing

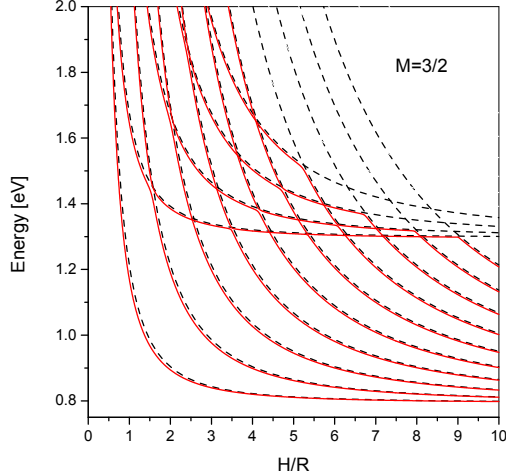


FIG. 4: (Color online) Same as Fig. 1 but for  $M = 3/2$ .

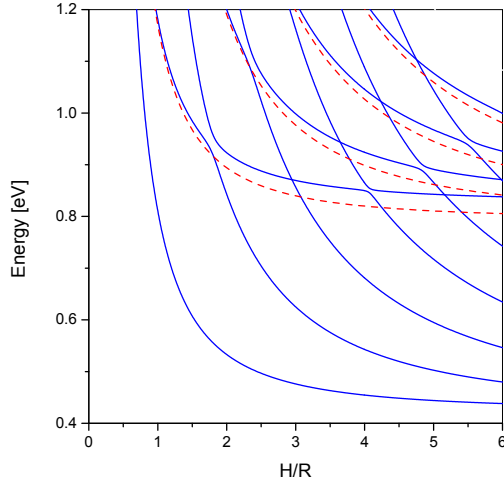


FIG. 5: (Color online) Energies of levels of size quantization for the quantum number  $|M| = 1/2$  (solid lines) and  $|M| = 3/2$  (dashed lines) in a PbSe nanorod of radius  $R = 20 \text{ \AA}$  and height  $H$  as functions of  $H/R$ .

quantum states of opposite parities at the apexes of 1D subbands [6]. When  $k_z \neq 0$  the two solutions mix. This mixing is fairly weak and can be considered as a perturbation of the subband dispersion relations described by the equations  $B = 0$  and  $C = 0$ . The structure of Eq. (5) suggests that this perturbation is linear in  $k_z$ . In the space of envelope wave functions  $k_z$  can be considered as the operator of the  $z$  component of the linear momentum in the momentum representation. The same operator in the coordinate representation is proportional to the first derivative with respect to  $z$ , or  $\partial/\partial z$ . The functions (4) are either

odd or even with respect to the transformation  $z \rightarrow H - z$ . The operator  $\partial/\partial z$  can only have non-vanishing matrix elements between the functions of different parity (under the transformation  $z \rightarrow H - z$ ). Thus, the levels originating from the lower quantum wire subband characterized in the zeroth order by odd (even)  $n_z$  cross with the levels originating from the upper quantum wire subband characterized by odd (even)  $n_z$  and anti-cross with the levels characterized by even (odd)  $n_z$ , provided that these subbands have the same quantum number  $|M|$ . Note, however, that, if the states in the first ( $n_c = 1$ ) quantum wire subband with a given  $|M|$  are characterized at  $k_z = 0$  by the equation  $B = 0$  so will the states from the third ( $n_c = 3$ ) subband. Therefore, the electron energy levels in nanorods originating from the first and the third quantum wire subbands characterized by the same quantum number  $|M|$  will always cross, and the checker board pattern will be broken for higher energies. This observation has been verified by numerical calculations.

To summarize, we have demonstrated that for most practical purposes the effect of the finite height of a lead salt nanorod on its electronic structure can be accounted for by sampling the subband dispersion dependencies of the infinite cylindrical quantum wire of the same radius at wave numbers  $k_z = \pi n_z/H$ , where  $H$  is the nanorod height and  $n_z$  is an integer. This approximation can fail if, for a given nanorod height, some of the energy levels originating from different quantum wire subbands characterized by the same absolute value  $|M|$  of the total angular momentum projection onto the quantum wire axis are close to one another. The levels would repel if the corresponding states are characterized by the numbers  $n_z$  of different parities and originate from subbands characterized by the same value of  $|M|$  and main quantum numbers of opposite parities, giving rise to the levels splitting.

This work was supported by the Research Corporation for Science Advancement (Award No. 20081), the Russian Foundation for Basic Research and the National Science Foundation (Grant No. HRD-0833178).

- 
- [1] X.G. Peng, L. Manna, W.D. Yang, J. Wickham, E. Scher, A. Kadavanich, and A.P. Alivisatos, *Nature* **404**, 59 (2000).
- [2] S. Acharya, U.K. Gautam, T. Sasaki, Y. Bando, Y. Golan, and K. Ariga, *J. Am. Chem. Soc.*



**130**, 4594 (2008).

- [3] J.M. Luther, H. Zheng, B. Sadtler, and A.P. Alivisatos, *J. Am. Chem. Soc.* **131**, 16851 (2009).
- [4] W.-K. Koh, A.C. Bartnik, F.W. Wise, and C.B. Murray, *J. Am. Chem. Soc.* **132**, 3909 (2010).
- [5] A. Rubin-Brusilovski, G. Maikov, D. Kolan, R. Vaxenburg, J. Tilchin, Y. Kauffmann, A. Sashchiuk, and E. Lifshitz, *J. Phys. Chem. C* **116**, 18983 (2012).
- [6] S.V. Goupalov, *Phys. Rev. B* **84**, 037303 (2011).
- [7] A.C. Bartnik, A.L. Efros, W.-K. Koh, C.B. Murray, and F.W. Wise, *Phys. Rev. B* **82**, 195313 (2010).
- [8] I. Kang and F.W. Wise, *J. Opt. Soc. Am. B* **14**, 1632 (1997).